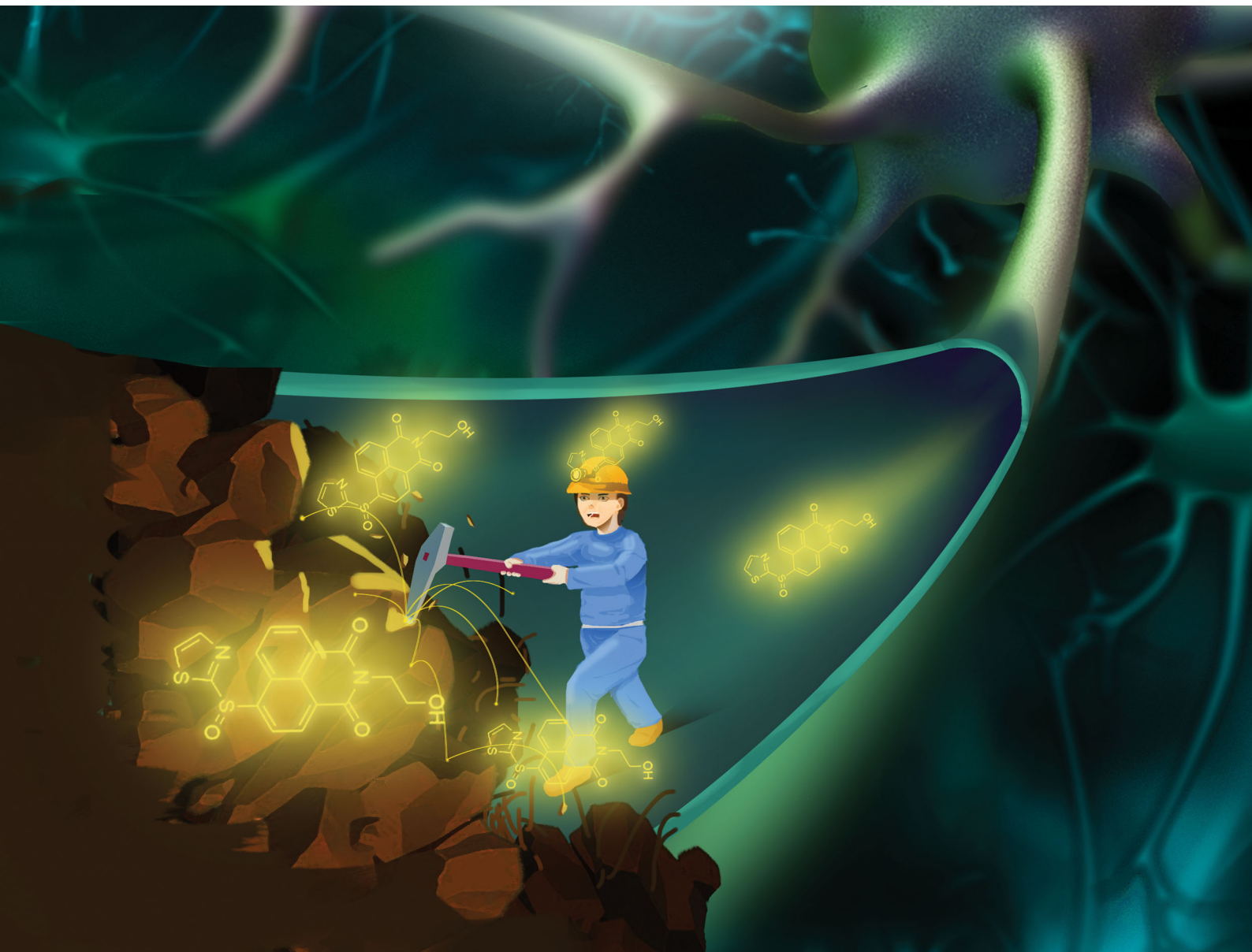


ChemComm

Chemical Communications

rsc.li/chemcomm



ISSN 1359-7345



Cite this: *Chem. Commun.*, 2020, **56**, 515

Received 2nd October 2019,
Accepted 27th November 2019

DOI: 10.1039/c9cc07753g

rsc.li/chemcomm

Understanding GSH flux in developing neurons is prerequisite to reveal its role in neuronal development but necessitates an ultra-sensitive assay. By systematically exploring key structural factors determining probe sensitivity in live cells, we developed a fluorogenic probe capable of imaging subtle GSH fluctuations in developing neurons.

Neuronal development refers to a series of complex processes involving proliferation, differentiation, migration, axon guidance and synapse formation,^{1–4} among which, the central challenge is to explain how axons and dendrites grow out to selectively synapse with their partners in order to establish a functional network.⁵ Studying the flux of key molecules during neuronal development may shed light on the molecular mechanisms by which complex nervous systems develop. It has recently been revealed that reactive oxygen species act as signaling molecules regulating neuronal development and function.^{6,7} However, little is known about glutathione (GSH) which is opposite in redox activity when compared to reactive oxygen species from a chemistry perspective, and in addition is involved in neuronal development.

To shed light on the role of GSH in neuronal development, it is essential to have a facile assay suitable for determining the flux with spatial resolution. Traditionally, biological GSH is determined with Ellman's reagent.⁸ This protocol necessitates cell lysis, therefore is not applicable for the detection of GSH in outgrowing axon or dendrites of developing neurons. Live-cell fluorescent imaging has the major advantage of providing

A fluorogenic probe for tracking GSH flux in developing neurons†

Haichao Zong,^{‡,ab} Jiayi Peng,^{‡,c} Xiao-Rong Li,^c Meng Liu,^{ab} Yongzhou Hu,^{id}^c Jia Li,^{ab} Yi Zang,^{*,ab} Xin Li,^{id}^c and Tony D. James^{id}^d

spatiotemporally resolved images of target biomolecules, and is emerging as an indispensable technique in cell biology. While commercial monochlorobimane can be used as a specific fluorescent probe for GSH. The labeling of GSH with monochlorobimane is glutathione *S*-transferases (GST) dependent.⁹ Consequently, intracellular GST levels and the affinity of monochlorobimane to these transferases are also important factors determining imaging results. Given the importance of GSH biology, there have been many new GSH probes developed in recent years. However, most of the research efforts were focused on improving probe reversibility,^{10–14} or to differentiate GSH from other biothiols,^{15–20} while improvements in probe sensitivity have been largely underexplored. Due to this missing link, most reported probes demonstrate only moderate (*ca.* ten fold) fluorescence changes in response to GSH, yielding relatively poor signal-to-background ratios, which could severely limit their application in the determination of subtle fluctuations of GSH involved in normal physiological processes, *e.g.* GSH flux in neuronal development. Given the relatively low levels of GSH in mature neurons,²¹ ultrasensitive probes capable of monitoring subtle GSH fluctuations are required. Herein, we report an approach to the optimization of GSH probes where both the stereoelectronic effect of the GSH recognition group, and probe physiochemical properties were considered in order to improve their intracellular sensitivity. This strategy uncovered GP5 with an excellent 6300 fold fluorogenic response towards GSH in aqueous solution, allowing the tracking of subtle fluctuations of GSH in developing neurons.

The sulfinyl functional group on an aromatic system is a good leaving group for S_NAr by stabilizing the Meisenheimer complex.²² We therefore reasoned that an optimized sulfinyl group may be an ideal GSH recognition group for probe development. Firstly, it can efficiently quench fluorophore fluorescence when incorporated into the usual “push” position of a push–pull fluorophore. Secondly, it may be nucleophilically substituted by GSH to trigger fluorescence turn-on. Thirdly, it is less reactive than Michael receptors used to couple proteins, and therefore should be friendlier to biological systems where proteins with free thiols are ubiquitous. We therefore set out to develop an

^a State Key Laboratory of Drug Research, Shanghai Institute of Materia Medica, Chinese Academy of Sciences, Shanghai 201203, China.

E-mail: yzang@simm.ac.cn

^b University of Chinese Academy of Sciences, Beijing 100049, China

^c College of Pharmaceutical Sciences, Zhejiang University, Hangzhou 310058, China.
E-mail: lixin81@zju.edu.cn

^d Department of Chemistry, University of Bath, Bath, BA2 7AY, UK

† Electronic supplementary information (ESI) available: Probe synthesis and characterization, cell imaging experiments, and supplementary figures. See DOI: [10.1039/c9cc07753g](https://doi.org/10.1039/c9cc07753g)

‡ These authors contributed equally to this work.



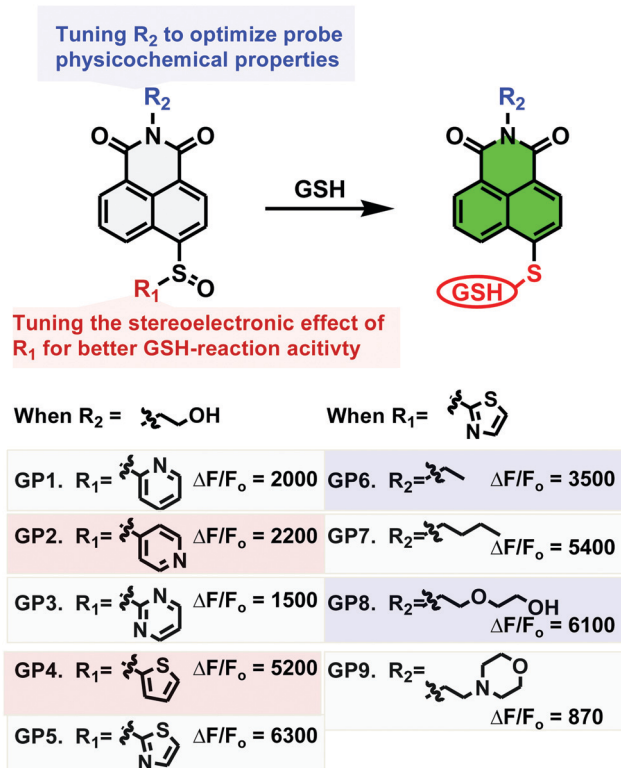


Fig. 1 Tuning the stereoelectronic effect and physicochemical property of sulfinyl naphthalimides for sensitive GSH probes. Designed probes (5 μM) were tested for their fluorogenic response towards GSH (2 mM) in PBS (10 mM, pH 7.4), and the degree of fluorescence increase ($\Delta F/F_0$) was compared.

ultrasensitive probe for GSH employing the sulfinyl group as the recognition trigger (Fig. 1).

Firstly, to investigate the impact of the stereoelectronic effect on the probes sensitivity, sulfinyl groups with various electron-withdrawing groups or sizes were incorporated into the 1,8-naphthalimide scaffold which belongs to the classical push–pull family of fluorophores. These probes are basically non-fluorescent in PBS (10 mM, pH 7.4), due to the lack of electron push–pull effect which is essential for the fluorescence response. When they were treated with GSH (2 mM) in PBS (10 mM, pH 7.4) to mimic the biological environment, all probes displayed fluorogenic responses, but with dramatically different sensitivity. As shown in Fig. S1 (ESI[†]) which represents probe emission spectra after 60 min of incubation with GSH, **GP4** and **GP5** bearing thienyl or thiazolyl group demonstrated the most dramatic fluorogenic response (5200-, and 6300-fold, respectively), while **GP1–GP3** bearing pyridyl or pyrimidyl moieties gave significantly decreased fluorogenic response (1500–2200 fold). Time-lapsed emission at 496 nm of these probes in response to GSH treatment displayed similar results with **GP4** and **GP5** being the most sensitive (Fig. S2, ESI[†]). These results suggest that steric hindrance caused by the sulfinyl group was particularly important in determining the probes sensitivity towards GSH. The electronic effect of the sulfinyl group on sensitivity is more complicated, with moderate electron-withdrawing effects being favoured.

To compare their sensitivity towards GSH in live cells, these probes were tested for their ability to image native GSH in primary cortex neurons (DIV2). As shown in Fig. S3 (ESI[†]), cells stained with **GP5** displayed the most dramatic intracellular fluorescence. This agrees well with the results obtained by solution-based screening. While unexpectedly, **GP4** displayed lower and **GP2** higher sensitivity for live cell imaging than they did in solution-based assays. This was presumably due to their different cell permeability which affects their actual intracellular concentrations. These results highlight the importance of cell-based screening as an indispensable complement for probe screening.

Having determined the thiazolyl sulfinyl moiety as the optimized functionality for sensing GSH, we then evaluated the effect of probe lipophilicity on the imaging activity. Since the side chain on the imide causes little effect on naphthalimide photophysical properties, we introduced chains with various degrees of lipophilicity to the imide. As showed in Fig. S4 and S5 (ESI[†]), probe **GP5** and **GP8** with hydrophilic 2-hydroxyethyl or 2-hydroxyethoxyethyl groups displayed the most dramatic fluorescent turn-on response (6300-, 6100-fold, respectively) towards GSH in aqueous solution, while **GP6** and **GP7** with ethyl or butyl substitution exhibited moderate fluorescent turn-on response (3500-, 5400-fold, respectively). Cell-based screening produced similar results, with **GP5** and **GP8** being the most sensitive probes, followed by **GP6** and **GP7** (Fig. S6, ESI[†]). However, the most hydrophilic **GP9** probe exhibited the weakest fluorescence turn-on response towards GSH in both solution-based and cell-based assays. These results when taken together, suggest that the balance between probe hydrophilicity and lipophilicity is crucial for improving probe sensitivity for live cell imaging.

The above optimization highlighted that probe **GP5** was a candidate for the fluorogenic detection of GSH in neurons. Before carrying it forward to study native GSH flux during neuronal development, its selectivity towards GSH was evaluated by measuring its fluorescence responses towards various bio-relevant analytes in PBS (10 mM, pH 7.4) (Fig. S7 and S8, ESI[†]). Among the various analytes tested at or above their bio-relevant concentrations, only GSH triggered the dramatic fluorogenic response of **GP5**. It should be noted that **GP5** is also active towards Cys and Hcy, but the sensitivity is low.

Then, the response of **GP5** towards various doses of GSH was evaluated. The **GP5** fluorescence intensity produces a single exponential increase in response to treatment with GSH (Fig. S9 and S10, ESI[†]), indicating pseudo first order kinetics. Noteworthy, **GP5** was found to be particularly sensitive to GSH in the range of 0–500 μM which covers the physiological cellular GSH levels in neurons.²¹ The detection limit of **GP5** towards GSH was calculated to be 0.11 μM according to literature methods (Fig. S11, ESI[†]).²³ These results collectively suggest good sensitivity of **GP5** towards low levels of GSH.

Having confirmed the sensitive and selective fluorogenic response of **GP5** towards GSH in aqueous solution, we further evaluated the selectivity towards GSH in live cells. First of all, **GP5** was shown to exhibit negligible cytotoxicity at working concentrations by the MTT assay (Fig. S12, ESI[†]). Then, its intracellular intensity change in response to pharmacological manipulation of GSH was explored. For this purpose, SH-SY5Y



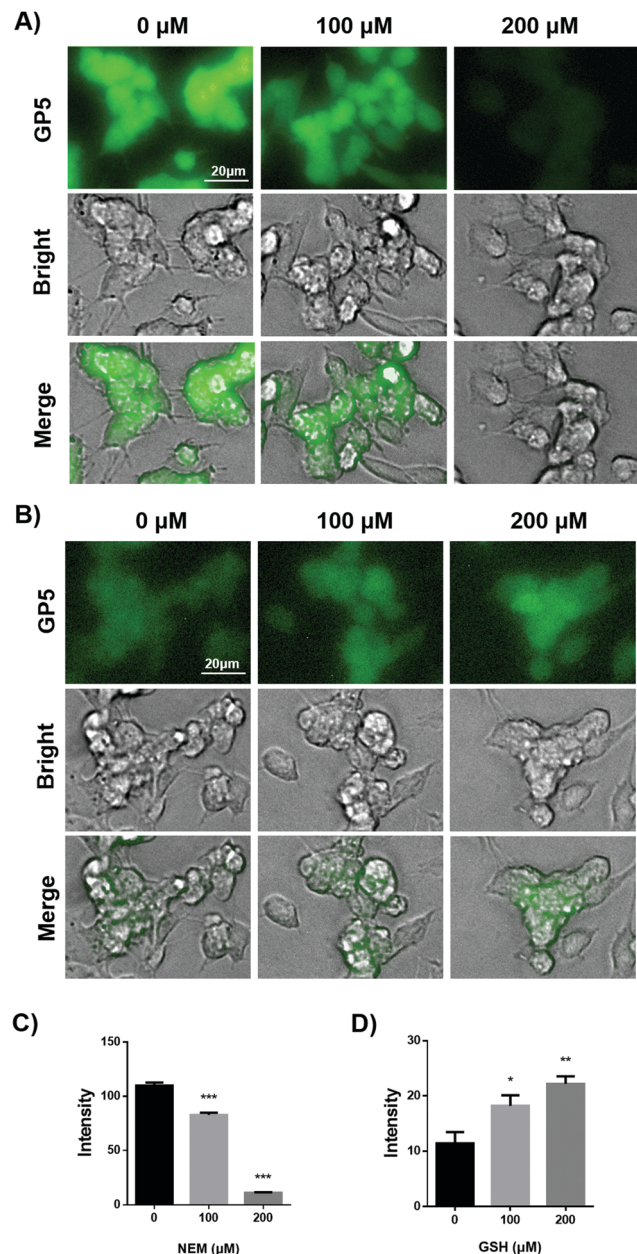


Fig. 2 **GP5** specifically and sensitively detects GSH in neuroblastoma SH-SY5Y cells. (A) Cells were incubated with NEM of indicated concentration for 30 min followed by being stained with **GP5** (10 μ M) for another 30 min, and then imaged. (B) Cells pretreated with NEM (200 μ M, 30 min) were incubated with GSH of indicated concentrations for another 30 min, and then stained with **GP5** (10 μ M) and imaged. (C) Quantified fluorescence intensities of cells as represented in panel (A). (D) Quantified fluorescence intensities of cells as represented in panel (B).

cells which are often used as *in vitro* models of neuronal function and differentiation were chosen as a model cell line.²⁴ When SH-SY5Y cells were incubated with **GP5** for 30 min, bright intracellular **GP5** fluorescence was observed, suggesting the presence of endogenous GSH (Fig. 2A). If SH-SY5Y cells were pretreated with *N*-ethylmaleimide (NEM), a GSH scavenger, for 30 min and then stained with **GP5**, the intracellular **GP5** fluorescence was observed to be significantly decreased compared with

the group without NEM pre-treatment. Furthermore, the intracellular **GP5** fluorescence was inversely dependent on the NEM dosage (Fig. 2A). These results suggest excellent selectivity of **GP5** towards GSH in live cells.

Furthermore, the sensitivity of **GP5** towards subtle change of GSH in live cells was investigated. SH-SY5Y cells were first treated with NEM (200 μ M) in-order to partially scavenge endogenous GSH. Then the cells were treated with low doses of exogenous GSH, followed by being stained with **GP5** (10 μ M) for 30 min. It was observed that the intracellular **GP5** fluorescence increased as the GSH dosage increased (Fig. 2B and D). Even a low gradient of 100 μ M exogenous GSH could induce significantly different intracellular **GP5** fluorescence. These results suggest that **GP5** should be sensitive enough to respond to subtle changes of cellular GSH.

Having confirmed the selectivity and sensitivity of **GP5** towards GSH in live cells, we then used the probe to evaluate GSH flux in primary cortex neurons during development. Cortex neurons were isolated from embryonic 16.5 (E 16.5) mice and planted onto a poly-lysine treated cell plate. During the first week of *in vitro* culture, cortex neurons acquired their characteristic morphology by a stereotyped sequence of developmental events divided into five stages. In the first stage, the GSH level was very low after neurons were planted onto the plate for 6 h (Fig. 3). However, the neuronal GSH level quickly elevated during the second stage and third stage, corresponding to neurite outgrowth and axon polarization. The GSH level maintained a high level after the start of polarization, then minimal fluctuation was observed during the final dendrites outgrowth and maturation process.

Dramatic up-regulation of intracellular **GP5** fluorescence was observed in primary cortex neurons before axon outgrowth. This may indicate the relevance of GSH to axonal guidance. To test this assumption, primary cortex neurons were treated with *L*-buthionine-sulfoximine (BSO), an inhibitor of the rate-limiting enzyme for GSH biosynthesis, for 40 h to reduce the intracellular GSH level. It should be noted that the long term treatment of BSO had no effect on the viability of these primary cortex

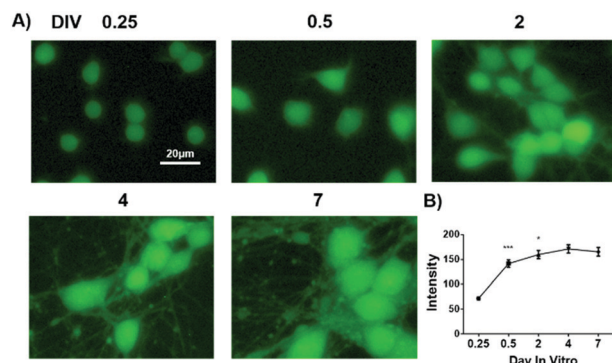


Fig. 3 Characterization of endogenous GSH fluctuation by **GP5** in primary cortex neurons during maturation. (A) Monitoring of endogenous GSH level in cultured primary cortex neurons derived from E16.5 mouse, for the five developmental stages by day *in vitro* (DIV)-0.25, 0.5, 2, 4, 7. (B) Quantified fluorescence intensities of different stages as represented in panel (A).

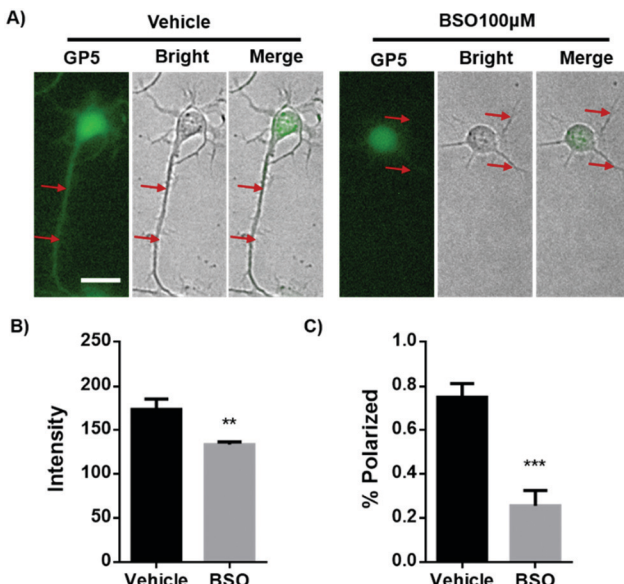


Fig. 4 Inhibiting GSH synthesis suppressed neuronal polarization in cultured primary cortex neurons. (A) Isolated primary cortex neurons from E16.5 day mice cortex were cultured *in vitro*, treated with BSO (100 μ M) for 40 h followed by staining with GP5 for 30 min. The axons are highlighted by arrows. (B) Quantified fluorescence intensities of cells as represented in panel (A). (C) Quantified percent of primary cortex neurons with the successful extension of a typical axon on neuronal polarization.

neurons (Fig. S13, ESI[†]). As expected, BSO treatment efficiently inhibited intracellular GSH level as shown by GP5 imaging (Fig. 4A and B). While interestingly, inhibiting GSH synthesis reduced the number of neurons possessing the typical elongated axon form. Actually, the percentage of the normally polarized neurons was decreased from 75% (control group without BSO treatment) to 25% (Fig. 4C), suggesting that GSH plays an indispensable role in axonal outgrowth and neuronal polarization.

In conclusion, by tuning the stereoelectronic effect of the GSH recognition group, and probe physicochemical properties, we have developed an fluorogenic probe for imaging GSH flux in developing neurons. The probe is a nonfluorescent sulfinyl naphthalimide but readily undergoes biocompatible reaction with GSH to produce a highly fluorescent sulphenyl naphthalimide. It is biology friendly and poses little toxicity to developing neurons. It is highly sensitive for imaging intracellular GSH. Facilitated by this probe, GSH flux throughout primary cortex neuron development has been determined. It was found that GSH levels are low at DIV1 and dramatically increased at DIV 2. Importantly, by using this probe, we have found that inhibiting GSH retards neuronal polarization, uncovering for the first time the indispensable role of GSH in neuronal polarization.

This work was supported by the National Natural Science Foundations of China (21778048, 81673489, 31871414, 81125023), Natural Science Foundation of Zhejiang Province,

China (LR18H300001). Shanghai Science and Technology Development Funds (19YF1457500). National Science & Technology Major Project “Key New Drug Creation and Manufacturing Program” (2018ZX09711002-010-004, 2018ZX09711002-007-002). TDJ wishes to thank the Royal Society for a Wolfson Research Merit Award.

Conflicts of interest

The authors declare no conflicts of interest.

Notes and references

- 1 M. S. Vieira, A. K. Santos, R. Vasconcellos, V. A. M. Goulart, R. C. Parreira, A. H. Kihara, H. Ulrich and R. R. Resende, *Biotechnol. Adv.*, 2018, **36**, 1946–1970.
- 2 A. P. Barnes and F. Polleux, *Annu. Rev. Neurosci.*, 2009, **32**, 347–381.
- 3 E. E. Govek, S. E. Newey and L. Van Aelst, *Genes Dev.*, 2005, **19**, 1–49.
- 4 C. G. Dotti, C. A. Sullivan and G. A. Bunker, *J. Neurosci.*, 1988, **8**, 1454–1468.
- 5 B. Alberts, A. Johnson, J. Lewis, M. Raff, K. Roberts and P. Walter, *Molecular Biology of the Cell*, Garland, 4th edn, 2002.
- 6 M. Olguín-Albuerne and J. Morán, *ASN Neuro*, 2015, **7**, 1759091415578712.
- 7 M. C. W. Oswald, N. Garnham, S. T. Sweeney and M. Landgraf, *FEBS Lett.*, 2018, **592**, 679–691.
- 8 P. Eyer, F. Worek, D. Kiderlen, G. Sinko, A. Stuglin, V. Simeon-Rudolf and E. Reiner, *Anal. Biochem.*, 2003, **312**, 224–227.
- 9 J. A. Cook, S. N. Iype and J. B. Mitchell, *Cancer Res.*, 1991, **51**, 1606–1612.
- 10 K. Umezawa, M. Yoshida, M. Kamiya, T. Yamasoba and Y. Urano, *Nat. Chem.*, 2017, **9**, 279–286.
- 11 Y. Takano, K. Hanaoka, K. Shimamoto, R. Miyamoto, T. Komatsu, T. Ueno, T. Terai, H. Kimura, T. Nagano and Y. Urano, *Chem. Commun.*, 2017, **53**, 1064–1067.
- 12 Z. Liu, X. Zhou, Y. Miao, Y. Hu, N. Kwon, X. Wu and J. Yoon, *Angew. Chem., Int. Ed.*, 2017, **56**, 5812–5816.
- 13 X. Jiang, J. Chen, A. Bajic, C. Zhang, X. Song, S. L. Carroll, Z.-L. Cai, M. Tang, M. Xue, N. Cheng, C. P. Schaa, F. Li, K. R. MacKenzie, A. C. M. Ferreon, F. Xia, M. C. Wang, M. Maletic-Savatic and J. Wang, *Nat. Commun.*, 2017, **8**, 16087.
- 14 H. Nie, J. Jing, Y. Tian, W. Yang, R. Zhang and X. Zhang, *ACS Appl. Mater. Interfaces*, 2016, **8**, 8991–8997.
- 15 L. Y. Niu, Y. S. Guan, Y. Z. Chen, L. Z. Wu, C. H. Tung and Q. Z. Yang, *J. Am. Chem. Soc.*, 2012, **134**, 18928–18931.
- 16 G. Yin, T. Niu, T. Yu, Y. Gan, X. Sun, P. Yin, H. Chen, Y. Zhang, H. Li and S. Yao, *Angew. Chem., Int. Ed.*, 2019, **58**, 4557–4561.
- 17 J. Zhang, X. Ji, H. Ren, J. Zhou, Z. Chen, X. Dong and W. Zhao, *Sens. Actuators, B*, 2018, **260**, 861–869.
- 18 H. Zhang, L. Xu, W. Chen, J. Huang, C. Huang, J. Sheng and X. Song, *ACS Sens.*, 2018, **3**, 2513–2517.
- 19 W. Chen, H. Luo, X. Liu, J. W. Foley and X. Song, *Anal. Chem.*, 2016, **88**, 3638–3646.
- 20 S.-Y. Lim, K.-H. Hong, D. I. Kim, H. Kwon and H.-J. Kim, *J. Am. Chem. Soc.*, 2014, **136**, 7018–7025.
- 21 X. Sun, A. Y. Shih, H. C. Johannsson, H. Erb, P. Li and T. H. Murphy, *J. Biol. Chem.*, 2006, **281**, 17420–17431.
- 22 D. W. Roberts, *Chem. Res. Toxicol.*, 1995, **8**, 545–551.
- 23 G. L. Long and J. D. Winefordner, *Anal. Chem.*, 1983, **55**, 712A–724A.
- 24 S. Pålman, S. Mamaeva, G. Meyerson, M. E. Mattsson, C. Bjelfman, E. Ortoft and U. Hammerling, *Acta Physiol. Scand., Suppl.*, 1990, **592**, 25–37.

